

AD-A103 274

AERONAUTICAL SYSTEMS DIV WRIGHT-PATTERSON AFB OH  
DEVELOPMENT AND APPLICATION OF A SUBSONIC TRIANGULAR VORTEX PAN--ETC(U)  
FEB 81 J C SPARKS

F/6 20/4

UNCLASSIFIED

ASD-TR-81-5005

NL

END  
DATE  
9 81  
DTIC

AD A103274

ASD-TR-81-5005

LEVEL

2

DEVELOPMENT AND APPLICATION OF A SUBSONIC TRIANGULAR VORTEX PANEL

John C. Sparks

Loads and Dynamics Branch  
Structures Division

DTIC  
S D  
AUG 25 1981  
H

February 1981

TECHNICAL REPORT ASD-TR-81-5005

Final Report for Period 1 September 1979 to 31 August 1980

Approved for public release; distribution unlimited

DEPUTY FOR ENGINEERING  
AERONAUTICAL SYSTEMS DIVISION  
AIR FORCE SYSTEMS COMMAND  
WRIGHT-PATTERSON AIR FORCE BASE, OHIO 45433

AMERICAN  
FILE COPY

81 8 25 010

NOTICE

When Government drawings, specifications, or other data are used for any purpose other than in connection with a definitely related Government procurement operation, the United States Government thereby incurs no responsibility nor any obligation whatsoever; and the fact that the government may have formulated, furnished, or in any way supplied the said drawings, specifications, or other data, is not to be regarded by implication or otherwise as in any manner licensing the holder or any other person or corporation, or conveying any rights or permission to manufacture use, or sell any patented invention that may in any way be related thereto.

This report has been reviewed by the Office of Public Affairs (ASD/PA) and is releasable to the National Technical Information Service (NTIS). At NTIS, it will be available to the general public, including foreign nations.

This technical report has been reviewed and is approved for publication.

John C. Sparks

JOHN C. SPARKS  
Aerospace Engineer

John H. Wafford

JOHN H. WAFFORD Chief  
Loads and Dynamics Branch  
Structures Division

FOR THE COMMANDER

Clovis L. Petrin, Jr.

CLOVIS L. PETRIN  
Chief, Structures Division

"If your address has changed, if you wish to be removed from our mailing list, or if the addressee is no longer employed by your organization please notify \_\_\_\_\_, W-PAFB, OH 45433 to help us maintain a current mailing list".

Copies of this report should not be returned unless return is required by security considerations, contractual obligations, or notice on a specific document.

AIR FORCE/56780/23 April 1981 - 180

REPORT DOCUMENTATION PAGE		READ INSTRUCTIONS BEFORE COMPLETING FORM
1. REPORT NUMBER <i>14</i> ASD-TR-81-5005	2. GOVT ACCESSION NO. <i>AD-A103274</i>	3. RECIPIENT'S CATALOG NUMBER
4. TITLE (and Subtitle)  DEVELOPMENT AND APPLICATION OF A SUBSONIC TRIANGULAR VORTEX PANEL	5. TYPE OF REPORT & PERIOD COVERED <i>9</i> Final Report 1 Sept 1979 - 31 August 1980	
7. AUTHOR(s)  John C. Sparks	6. CONTRACT OR GRANT NUMBER(s)	
9. PERFORMING ORGANIZATION NAME AND ADDRESS  Structures Division (ASD/ENFS) Directorate of Flight Systems Engineering Wright-Patterson AFB OH 45433	10. PROGRAM ELEMENT, PROJECT, TASK AREA & WORK UNIT NUMBERS <i>16</i> 61000000	
11. CONTROLLING OFFICE NAME AND ADDRESS  Aeronautical Systems Division (ASD) Wright-Patterson AFB OH 45433	12. REPORT DATE <i>11</i> February 1981	
14. MONITORING AGENCY NAME & ADDRESS (if different from Controlling Office)	13. NUMBER OF PAGES <i>52</i>	
16. DISTRIBUTION STATEMENT (of this Report)	15. SECURITY CLASS. (of this report)  UNCLASSIFIED	
Approved for public release; distribution unlimited.	15a. DECLASSIFICATION/DOWNGRADING SCHEDULE	
17. DISTRIBUTION STATEMENT (of the abstract entered in Block 20, if different from Report)	DTIC S E AUG 25 1981 H	
18. SUPPLEMENTARY NOTES  Approved for public release; IAW AFR 190-17.		
19. KEY WORDS (Continue on reverse side if necessary and identify by block number)	Airloads Aerodynamic Loading Potential Flow Subsonic Flow Perturbation Method Paneling Method Vortex Panel Singularity Method	
20. ABSTRACT (Continue on reverse side if necessary and identify by block number)	Paneling methods are approximate techniques for solving flow problems over wings and bodies. Vortex panels are used to model flow over wings and other lifting surfaces. The author develops a triangular vortex panel having a vorticity distribution that can vary in magnitude and direction. This panel is used to predict the pressure distribution on a rectangular and a swept-back wing in subsonic flow. Lift distributions obtained compare favorably to Anderson's solution and wind tunnel results.	

FOREWORD

This report was prepared by Mr. John C. Sparks of the Loads and Dynamics Branch (ENFSL), Structures Division (ENFS), Aeronautical Systems Division (ASD), Wright-Patterson Air Force Base, Ohio. The work was accomplished to help fulfill the requirements for the degree of Master of Science at the Air Force Institute of Technology.

Appreciation is extended to my advisor, Major Stephen J. Koob of the Department of Aeronautics and Astronautics, Air Force Institute of Technology and to James R. Snyder of ASD/XRHI for his valuable suggestions. Appreciation is also extended to Capt. Ron Luther who found a programming error in the original computer code. The elimination of this error vindicated the theory and made this report possible.

Accession for	
NTIS GRISI	<input type="checkbox"/>
DTIC TAB	<input type="checkbox"/>
Unpublished	<input type="checkbox"/>
Justification	<input type="checkbox"/>
By	
Distribution	
Availability Codes	
Avail and/or	
Dist	Special
A	

Contents

	Page
<b>Abstract</b> .....	ix
<b>I. Introduction</b> .....	1
Background.....	1
Problem Statement.....	1
Approach.....	2
<b>II. Panel Derivation</b> .....	4
Geometry.....	4
Singularity Strength Distribution.....	4
Consequence of the Helmholtz Condition.....	6
Bilinear Coefficients in Terms of Corner Vorticity.....	6
Mathematical Continuity.....	9
Application of the Biot-Savart Law.....	9
Summary.....	13
<b>III. Panel Assembly</b> .....	14
Panel Numbering.....	14
Number of Unknowns, Boundary Conditions and Numbering.....	14
Boundary Conditions.....	14
Unknown Numbering Scheme.....	17
Solving for the Corner Vorticities.....	19
Control Point Equations.....	19
Edge Continuity Conditions.....	20
Compressibility.....	21
Matrix Formulation.....	22
Solution.....	22
Forces and Moments.....	23
<b>IV. Results</b> .....	25
Rectangular Wing.....	25
Swept Wing.....	25

Contents

	Page
V. Conclusions and Recommendations.....	32
Conclusions.....	32
Recommendations.....	32
Appendix A: Evaluation of the Panel Integrals.....	33
Appendix B: Simple Wake Model.....	40
Bibliography.....	43

List of Figures

Figure	Page
1 Panel Geometry and Corner Point Numbering Scheme	5
2 A Paneling Arrangement and Associated Numbering Scheme for a 16 Panel Wing	15
3 Unknown Numbering Scheme for a 9 Panel Wing	18
4 $C_L$ Versus Span Station for a Rectangular Wing; $AR = 8, \alpha = 5^\circ$ .	26
5 $X_{cp}/c$ Versus Span Station for a Rectangular Wing; $AR = 8, \alpha = 5^\circ$ .	27
6 $\gamma$ Strength Distribution at the Root Chord of a Rectangular Wing; $AR = 8, \alpha = 5^\circ$ .	28
7 $C_L$ Versus Span Station for a Sweptback Untapered Wing; $AR = 4.5, \Lambda = 40^\circ, \alpha = 5^\circ$ .	30
8 $X_{cp}/c$ Versus Span Station for a Sweptback Untapered Wing; $AR = 4.5, \Lambda = 40^\circ, \alpha = 5^\circ$ .	31
9 Semi-Infinite Strip R Used in Integral Evaluation	34
10 Wake Model	41

List of Symbols

## Symbol

$\alpha$	.....angle of attack
$\vec{\omega}$	.....vorticity vector
$\delta(x,y), \gamma(x,y), 0$	.....Components of $\vec{\omega}$
$A, B, C$	.....coefficients of the assumed "bilinear" form for $\gamma$
$D, E, F$	.....coefficients of the assumed "bilinear" form for $\delta$
$x_i, y_i$	.....panel corner points
$\delta_i, \gamma_i$	.....corner vorticity values
$x, y, z$	.....chordwise, spanwise, and normal coordinates, respectively
$\Gamma$	.....straight line segment
$\vec{s}$	.....control point in the plane $z = 0$
$u, v, w$	.....perturbation velocities in the respective $x, y$ , and $z$ directions
$\hat{i}, \hat{j}, \hat{k}$	.....unit vectors in the respective $x, y$ , and $z$ directions
$R$	.....region of integration
$M$	.....number of chordwise panels or slope (Appendix A only)
$N$	.....number of spanwise panels
$\Lambda$	.....leading edge slope (Section III)
$(\theta_j)$	.....column vector of corner vorticities
$(A_{ij})$	.....coefficient matrix premultiplying $(\theta_j)$
$M_\infty$	.....free stream Mach number
$V_\infty$	.....free stream velocity

List of Symbols

## Symbol

dc/dx	.....camber slope
$\gamma$	.....ratio of specific heats (eqs 3.30 and 3.31 only)
$f_i(x, y)$	.....integrands obtained through application of the Biot-Savart Law
$F_i$	.....improper integrals of the form

$$\lim_{L \rightarrow \infty} \int_{y_0}^{y_1} \int_{-\infty}^L f_i(x, y) dx dy \quad i = 1, \dots, 5$$

$$(y - b)/M$$

$s_i$	.....strip function
$I_i$	.....integral over a triangular region
$c_p$	.....pressure coefficient
$c_L$	.....local lift coefficient
$c_M$	.....local pitching moment coefficient

Subscripts and Superscripts

L	.....leading triangle
T	.....trailing triangle

ABSTRACT

Paneling methods are approximate techniques for solving flow problems over wings and bodies. Vortex panels are used to model flow over wings and other lifting surfaces. The author develops a triangular vortex panel having a vorticity distribution that can vary in magnitude and direction. This panel is used to predict the pressure distribution on a rectangular and a sweptback wing in subsonic flow. Lift distributions obtained compare favorably to Anderson's solution and wind tunnel results.

DEVELOPMENT AND APPLICATION  
OF A SUBSONIC TRIANGULAR  
VORTEX PANEL

I. Introduction

Background

Paneling methods are approximate techniques for solving linearized subsonic and supersonic potential flow problems over wings and bodies. Panels in use today incorporate singularity distributions of the source, vortex, and doublet types. Source panels are often used to model bodies and other non-lifting surfaces and to model thickness of lifting surfaces. Vortex panels are used to model either lifting or non-lifting surfaces. In a typical problem, the airplane is represented by a finite number of panels. Each panel is a singularity distribution of unknown strength that models some part of the aerodynamic surface. These unknown strengths are determined by applying the flow tangency boundary conditions at or near the aerodynamic surfaces. Once the strengths are known, the perturbation velocities can be computed. These are substituted into the Bernoulli equation to obtain the pressure distribution and the corresponding aerodynamic forces and moments.

Problem Statement

In many current paneling methods, the orientation of the vorticity vector is fixed on the panel (Ref 6 and Ref 8). This leads to unacceptable errors in some cases. The purpose of this study is to

derive a subsonic triangular panel having a vorticity distribution that can vary both in magnitude and direction. A panel system is assembled and used to predict the pressure distribution on a planform. Since the computations involved are too lengthy to be performed by hand, a computer code was developed to apply the panels to planar wings.

Approach

The subsonic triangular panel is derived in Section II. The Biot-Savart Law is used to compute the induced velocity at a point due to an assumed bilinear vorticity distribution on the panel. This expression formulates the induced velocity in terms of panel geometry and unknown corner point vorticity.

Section III presents methodology for panel system assembly. Numbering schemes are developed for panels and the unknown corner point vorticities. Planform boundary conditions are applied which reduce the number of unknowns and the remaining unknowns are solved for by formulating a linear system of equations. This system consists of control point equations (one per panel) and a number of edge continuity conditions. The linearized form of the flow tangency boundary condition is then used to effect the solution. Once the corner vorticities are known, the vorticity at any point on the planform can be obtained. Finally, induced velocities and corresponding pressures can be calculated from the known vorticity.

Section IV presents program predictions for a rectangular wing

ASD-TR-81-5005

which are compared against Anderson's solution (Ref 1:9-16). Predictions are also presented for a swept untapered wing which are compared against wind tunnel tests (Ref 4:92).

Section V concludes the report and makes recommendations for the improvement of the aerodynamic model.

II. Panel Derivation

This section presents the development of the subsonic triangular panel. The goal is to derive an expression for the induced velocity at an arbitrarily chosen point in the  $xy$  plane due to an assumed bilinear vorticity distribution on the panel.

Geometry

The first step in panel development is the definition of panel geometry. Initially assume the panel is a trapezoid lying in the  $xy$ -plane and having two edges parallel to the  $x$ -axis. It is then subdivided into two triangles having a common side that joints the upper left hand corner to the lower right hand corner. The panel is oriented so that the root and tip chords lie parallel to the free stream flow direction at  $\alpha = 0$ . Figure 1 depicts the panel geometry, corner point numbering scheme, and coordinate system.

Singularity Strength Distribution

The general form of the singularity strength distribution on the panel will be

$$\tilde{\omega}(x, y) = \delta(x, y)\hat{i} + \gamma(x, y)\hat{j} \quad (2.1)$$

where  $\delta$  and  $\gamma$  are continuous functions of  $x$  and  $y$ . For the purpose of this study,  $\delta$  and  $\gamma$  are assumed to have the "bilinear" forms

$$\delta(x, y) = F + Dx + Ey \quad (2.2)$$

$$\gamma(x, y) = A + Bx + Cy \quad (2.3)$$

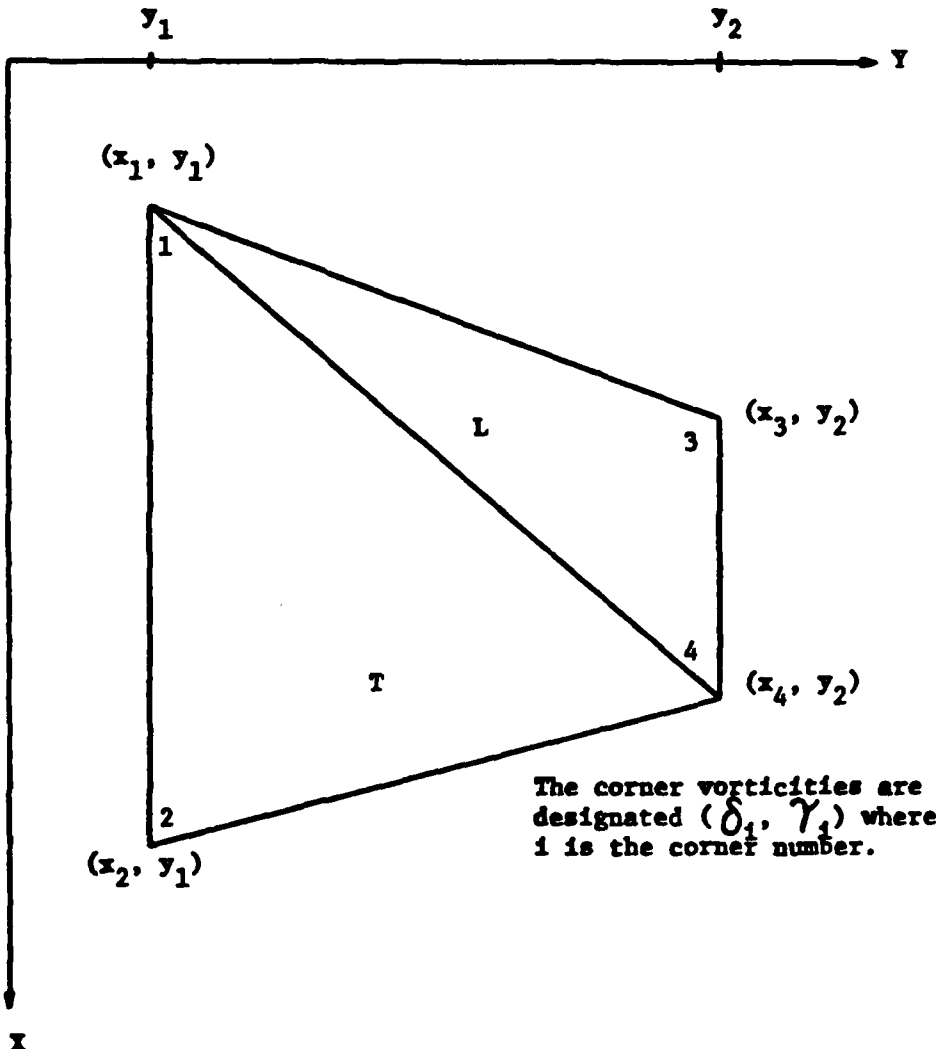


Figure 1. Panel Geometry and Corner Point Numbering Scheme

where the coefficients A, B, C, D, F, D and E are yet to be determined constants. These constants will be expressed as functions of the panel geometry and the unknown singularity strengths at the corner points.

#### Consequence of the Helmholtz Condition

The vorticity distribution  $\bar{\omega}(x, y)$  is required to satisfy the Helmholtz condition that vorticity must be preserved in the fluid. Thus,

$$\nabla(\delta_j + \gamma_j) = 0 \quad (2.4)$$

on the panel. If  $\delta$  and  $\gamma$  have the forms (2.2) and (2.3), respectively, then

$$\partial(F + Dx + Ey)/\partial x + \partial(A + Bx + Cy)/\partial y = 0 \quad (2.5)$$

which implies

$$D = -C \quad (2.6)$$

such that

$$\delta(x, y) = F - Cx + Ey \quad (2.7)$$

The formulation could be continued in terms of the bilinear coefficients. However, it is conventional to express them in terms of panel corner point vorticities.

#### Bilinear Coefficients in Terms of Corner Vorticity

In the ensuing discussion, the subscript L refers to the leading triangle and the subscript T refers to the trailing triangle.

The  $\gamma$  component of vorticity (eq (2.3)) is assigned the unknown values  $\gamma_1, \gamma_3, \gamma_4$  at the corners  $(x_1, y_1), (x_3, y_2)$ , and  $(x_4, y_2)$  of the leading triangle. This leads to the following system of three

equations in  $A_L$ ,  $B_L$  and  $C_L$ :

$$\gamma_1 = A_L + B_L x_1 + C_L y_1 \quad (2.8)$$

$$\gamma_3 = A_L + B_L x_3 + C_L y_2 \quad (2.9)$$

$$\gamma_4 = A_L + B_L x_4 + C_L y_2 \quad (2.10)$$

The system has the solution:

$$A_L = y_2 \gamma_1 / (y_2 - y_1) + [(y_1 x_4 - x_1 y_2) / (y_2 - y_1)]$$

$$\gamma_3 / (x_3 - x_4) + [(x_1 y_2 - y_1 x_3) / (y_2 - y_1)]$$

$$\gamma_4 / (x_3 - x_4) \quad (2.11)$$

$$B_L = (\gamma_3 - \gamma_4) / (x_3 - x_4) \quad (2.12)$$

$$C_L = -\gamma_1 / (y_2 - y_1) + [(x_1 - x_4) / (y_2 - y_1)] \gamma_3 /$$

$$(x_3 - x_4) + [(x_3 - x_1) / (y_2 - y_1)] \gamma_4 / (x_3 - x_4) \quad (2.13)$$

Since  $D_L = -C_L$ , only two corner conditions may be used to solve for  $F_L$  and  $E_L$  in the  $\delta$  component eq (2.7). Assigning the values  $\delta_1$  and  $\delta_3$  at the corners  $(x_1, y_1)$  and  $(x_3, y_2)$  leads to

$$\delta_1 + C_L x_1 = E_L y_1 + F_L \quad (2.14)$$

$$\delta_3 + C_L x_3 = E_L y_2 + F_L \quad (2.15)$$

and

$$k_L = (\delta_1 - \delta_3) / (y_1 - y_2) + [(x_1 - x_3) / (y_1 - y_2)] c_L \quad (2.16)$$

$$r_L = (y_1 \delta_3 - y_2 \delta_1) / (y_1 - y_2) + [(y_1 x_3 - x_1 y_2) / (y_1 - y_2)] c_L \quad (2.17)$$

In a similar way, the trailing triangle coefficient equations are obtained as follows:

$$A_T = y_1 \gamma_4 / (y_1 - y_2) + [(y_2 x_1 - x_4 y_1) / (y_1 - y_2)] \gamma_2 / (x_2 - x_1) \quad (2.18)$$

$$B_T = (\gamma_2 - \gamma_1) / (x_2 - x_1) \quad (2.19)$$

$$C_T = -\gamma_4 / (y_1 - y_2) + [(x_4 - x_1) / (y_1 - y_2)] \gamma_2 / (x_2 - x_1) + [(x_2 - x_4) / (y_1 - y_2)] \gamma_1 / (x_2 - x_1) \quad (2.20)$$

$$k_T = (\delta_2 - \delta_4) / (y_1 - y_2) + [(x_2 - x_4) / (y_1 - y_2)] c_T \quad (2.21)$$

$$r_T = (y_1 \delta_4 - y_2 \delta_2) / (y_1 - y_2) + [(y_1 x_4 - x_2 y_2) / (y_1 - y_2)] c_T \quad (2.22)$$

where  $E_T$  and  $F_T$  have been expressed in terms of (as functions of)  $\bar{\omega}$  components at corners 2 and 4.

#### Mathematical Continuity

The bilinear vorticity distribution is continuous on each triangular region. In addition, the  $\gamma$  component has been made to be continuous throughout the planform by the representation in terms of corner values. This can be demonstrated as follows. Let  $\Gamma$  be the boundary shared by any two adjacent triangles. Then  $\Gamma$  is a straight line segment and can be described by a linear expression (i.e.,  $y$  in terms of  $x$  or  $x$  in terms of  $y$ ). The  $\gamma$  distribution on each of the adjacent triangles will degenerate to a linear function of a single variable upon substitution of this expression. Both functions assume the same  $\gamma$  values at the endpoints of  $\Gamma$ . Since only two points are needed to determine a straight line or a linear form, we have  $\gamma$  matching identically on  $\Gamma$ .

The  $\delta$  component has breaks in continuity throughout the planform. This is a consequence of applying the Helmholtz condition (eq (2.4)) which eliminated the constant  $D$  and expressing the remaining two unknowns in terms of two  $\delta$  corner values, out of a possible three. The  $\delta$  component is continuous on panel leading and trailing edges since it is on these edges that common  $\delta$  values are assumed at the endpoints. The  $\delta$  component is discontinuous on panel diagonals.

#### Application of the Biot-Savart Law

Let  $\bar{\omega}(\bar{x})$  be a vorticity distribution defined on a finite region  $R$  in the  $xy$  plane. Let  $\$$  be a fixed point (control point) in the plane.

The velocity induced at  $\vec{s}$  due to the distribution on  $R$  is given by the Biot-Savart Law (Ref 5:526-528):

$$4\pi\vec{v}(\vec{s}) = \iint_R [\vec{\omega}(\vec{r}) \times (\vec{s} - \vec{r})] / |\vec{s} - \vec{r}|^3 dR \quad (2.23)$$

Suppose the control point  $\vec{s}$  is located at the origin of the coordinate system. Note that this can be done by performing a simple translation of the plane. Then,

$$\vec{s} = (0, 0, 0) \quad (2.24)$$

$$\vec{s} - \vec{r} = (0, 0, 0) - (x, y, 0) = (-x, -y, 0) \quad (2.25)$$

Assuming the distribution has the form (2.1),

$$\vec{\omega} \times (\vec{s} - \vec{r}) = [x\gamma - y\delta] \vec{k} \quad (2.26)$$

where  $\vec{k}$  is the unit vector normal to the  $xy$ -plane. Substituting the expressions (2.25) and (2.26) into eq (2.23) yields:

$$4\pi v(0, 0, 0) = \iint_R (x\gamma - y\delta) / (x^2 + y^2)^{3/2} dR \quad (2.27)$$

Where  $v$  is the normal velocity component induced at the origin.

Substituting the expressions for  $\gamma$  (2.3) and  $\delta$  (2.7) into eq (2.27) yields:

$$4\pi v = \iint_R (Ax + Bx^2 + 2Cxy - Ey^2 - Fy) / (x^2 + y^2)^{3/2} dR \quad (2.28)$$

where  $R$  is taken as the region defined by a trapezoidal panel.

Let  $R_L$  and  $R_T$  be the subregions of  $R$  which correspond to the lead-

ing and trailing triangles. The coefficients A, B, C, F, and E remain constant on each subregion and eq (2.28) is rewritten as:

$$4\pi v = A_L I_1^L + A_T I_1^T + B_L I_2^L + B_T I_2^T + 2C_L I_3^L + 2C_T I_3^T - F_L I_4^L - F_T I_4^T - E_L I_5^L - E_T I_5^T \quad (2.29)$$

where

$$I_3^L, T = \iint_{R_L, T} (x/(x^2 + y^2)^{3/2}) dR \quad (2.30)$$

$$I_2^L, T = \iint_{R_L, T} (x^2/(x^2 + y^2)^{3/2}) dR \quad (2.31)$$

$$I_3^L, T = \iint_{R_L, T} (xy/(x^2 + y^2)^{3/2}) dR \quad (2.32)$$

$$I_4^L, T = \iint_{R_L, T} (y/(x^2 + y^2)^{3/2}) dR \quad (2.33)$$

$$I_5^L, T = \iint_{R_L, T} (y^2/(x^2 + y^2)^{3/2}) dR \quad (2.36)$$

Evaluation of these integrals may be found in Appendix A. Substitution of the expressions for  $A_L$  through  $E_T$  and collecting coefficients of the unknowns ( $\delta_1, \delta_2, \delta_3, \delta_4, \gamma_1, \gamma_2, \gamma_3$ , and  $\gamma_4$ ) yields, after considerable algebraic manipulation,

$$\begin{aligned}
4\pi v = & [(y_2^L - I_3^L)/(y_1 - y_2)] \delta_1 + \\
& [(y_2 I_4^T - I_5^T)/(y_1 - y_2)] \delta_2 + \\
& [(I_5^L - y_1 I_4^L)/(y_1 - y_2)] \delta_3 + \\
& [(I_5^T - y_1 I_4^T)/(y_1 - y_2)] \delta_4 + \\
& [(x_4 y_1 - y_2 x_2) I_1^T - (x_2 - x_1) y_2 I_1^L - \\
& (y_1 - y_2) I_2^T + (x_2 - x_1) K_L + \\
& (x_2 - x_4) K_T)/((x_2 - x_1)(y_1 - y_2))] \gamma_1 + \\
& [(y_2 x_1 - x_4 y_1) I_1^T + (y_1 - y_2) I_2^T + \\
& (x_4 - x_1) K_T)/((y_1 - y_2)(x_2 - x_1))] \gamma_2 + \\
& [(y_1 x_4 - x_1 y_2) I_1^L + (y_2 - y_1) I_2^L + \\
& (x_1 - x_4) K_L)/((y_2 - y_1)(x_3 - x_4))] \gamma_3 + \\
& [(x_1 y_2 - y_1 x_3) I_1^L - (x_3 - x_4) y_1 I_1^T - \\
& (y_2 - y_1) I_2^L + (x_3 - x_1) K_L + (x_3 - x_4) K_T)/ \\
& ((y_2 - y_1)(x_3 - x_4))] \gamma_4 \quad (2.35)
\end{aligned}$$

where

$$k_L = 2I_3^L - [(x_1 - x_3)/(y_1 - y_2)]I_5^L - \\ [(y_1x_3 - x_1y_2)/(y_1 - y_2)]I_4^L \quad (2.36)$$

$$k_T = 2I_3^T - [(x_2 - x_4)/(y_1 - y_2)]I_5^T - \\ [(y_1x_4 - x_2y_2)/(y_1 - y_2)]I_4^T \quad (2.37)$$

Summary

Expression (2.35) is the normal velocity induced at the origin of the  $xy$  plane by a trapezoidal vorticity panel. This velocity is due to a bilinear vorticity distribution which satisfies the Helmholtz condition eq (2.4).

### III. Panel Assembly

This section presents the panel assembly procedures needed to model a wing. The goal is to develop the methodology required to predict the pressure distribution and associated forces and moments on a wing.

#### Panel Numbering

Figure 2 illustrates a paneling arrangement and associated numbering scheme for a 16 panel wing. The panels are numbered consecutively in the chordwise direction starting with the inboard leading edge panels and terminating with the outboard trailing edge panels.

#### Number of Unknowns, Boundary Conditions and Numbering

Let  $M$  be the number of chordwise panels and  $N$  be the number of spanwise panels. These are defined using  $M + 1$  chordwise cuts and  $N + 1$  spanwise cuts. Each intersection determines a panel corner point. Since there are two unknown components at each corner point, the total number of unknowns is given by:

$$2(M + 1)(N + 1) \quad (3.1)$$

#### Boundary Conditions

Two boundary conditions are imposed on the wing panel system. These reduce the number of unknowns and improve the physical modeling of the flow field.

The Kutta condition (Ref 5:390-399)

The z axis is normal to the wing planform.

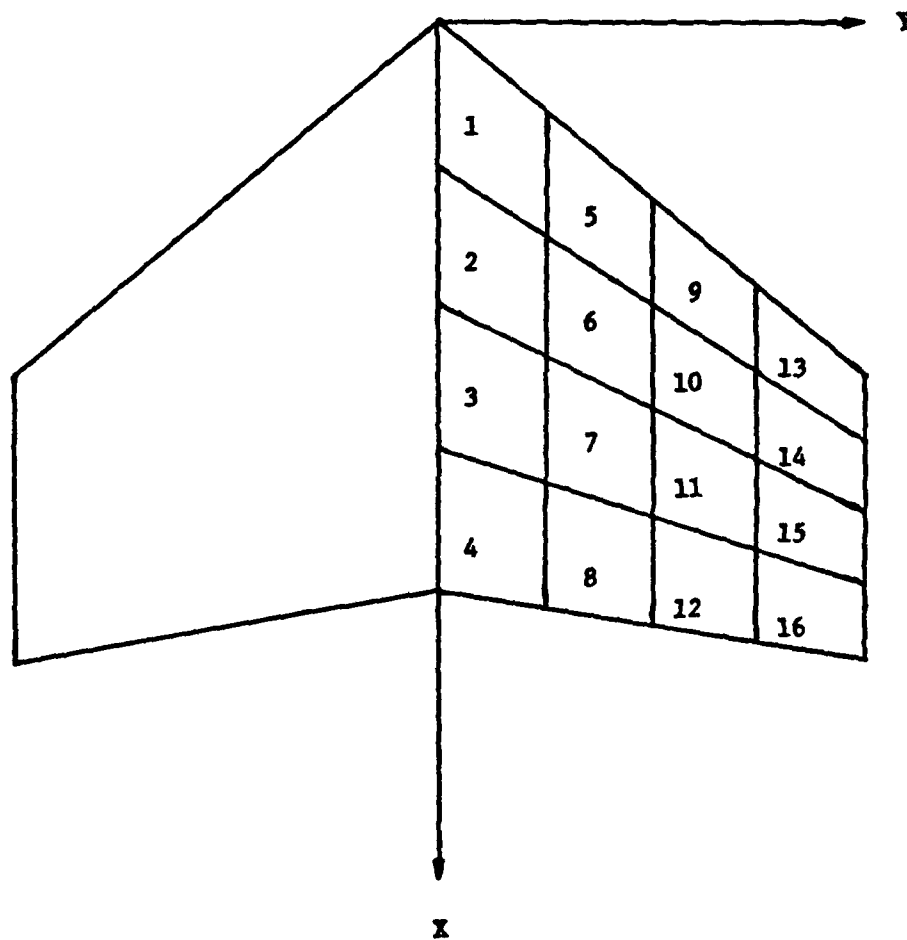


Figure 2. A Paneling Arrangement and Associated Numbering Scheme for a 16 Panel Wing

$$\gamma(x, y) = 0 \quad (3.2)$$

is imposed at all corner points on the wing trailing and tip edges. Since the  $\gamma$  component of vorticity eq (2.2) is both linear and continuous on these edges, the Kutta condition is satisfied identically. The Kutta condition reduces the total number of unknowns by:

$$M + N + 1 \quad (3.3)$$

(NOTE: The point defining the intersection of the trailing and tip edges is common to both.)

A historically acceptable boundary condition (an outgrowth of Prandtl's lifting-line theory (Ref 5:535-567)) is for the vorticity vector to lie tangent to the wing leading edge. This boundary condition initially orients the vorticity vector so that a positive circulation is produced. The boundary condition is imposed at all leading edge corner points and can be written:

$$\gamma/\delta = \Lambda \quad (3.4)$$

or

$$\delta = \gamma/\Lambda \quad (3.5)$$

where  $\Lambda$  is the leading edge slope at the corner point. It reduces the total number of unknowns by:

$$N + 1 \quad (3.6)$$

and the total number of unknowns becomes:

$$2MN + M \quad (3.7)$$

after imposing the two boundary condition equations (3.2) and (3.5).

Since the wing is symmetric about the x-axis, it may seem logical to impose a boundary condition at the wing root chord. However, setting

$$\delta = 0 \quad (3.8)$$

at the centerline is redundant for rectangular wings and leads to an ill-conditioned system once planform symmetry is considered.

#### Unknown Numbering Scheme

Figure 3 illustrates the unknown numbering scheme for a 9 panel wing with applied boundary conditions. The paneling arrangement of Figure 3 is chosen because it represents the smallest number of panels needed to illustrate interior panels and panels having boundary conditions. Let  $i$  be the panel number of an interior panel. Then the following numbers (in terms of  $i$ ,  $M$ , and  $N$ ) are assigned to the eight unknown corner vorticity components:

$$(\delta_1) \quad i - 1 \quad (3.9)$$

$$(\delta_2) \quad i \quad (3.10)$$

$$(\delta_3) \quad i + M - 1 \quad (3.11)$$

$$(\delta_4) \quad i + M \quad (3.12)$$

The unknown corner  $\delta$ 's are denoted by "-" and the  $\gamma$ 's by "=".

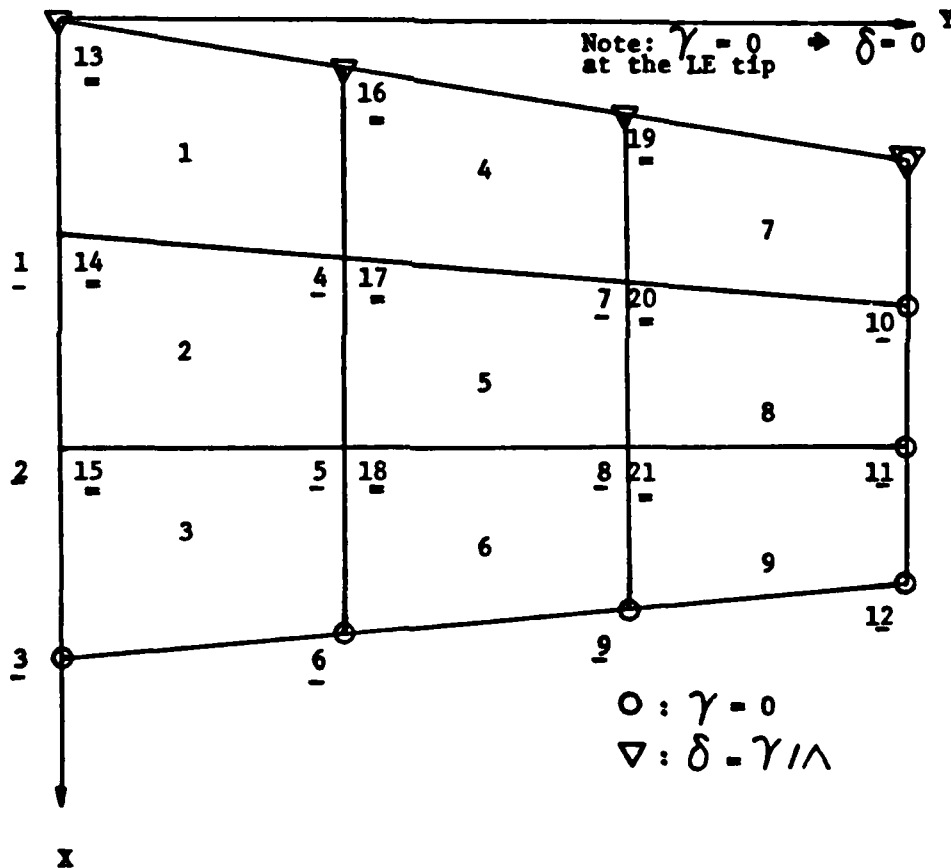


**Figure 3. Unknown Numbering Scheme for a 9 Panel Wing**

$$(\gamma_1) MN + M + 1 \quad (3.13)$$

$$(\gamma_2) MN + M + 1 + 1 \quad (3.14)$$

$$(\gamma_3) MN + 2M + 1 \quad (3.15)$$

$$(\gamma_4) MN + 2M + 1 + 1 \quad (3.16)$$

#### Solving for the Corner Vorticities

The total number of unknowns (after the boundary conditions are applied) is given by eq (3.7) which also specifies the number of conditions needed to solve for the corner vorticities. Two types of conditions will be used; control point conditions and edge or point continuity conditions.

#### Control Point Equations

Control point equations are obtained using eq (2.35). The velocity component is computed for one point (control point) on each panel comprising the wing.

Let  $(x_i, y_i)$  be the control point on panel i. To obtain the contribution to  $w_i$  due to panel j, express the coordinates of panel j in a coordinate system with  $(x_i, y_i)$  at the origin. This is done by performing a translation in the  $z = 0$  plane:

$$\begin{aligned} x' &= x - x_i \\ y' &= y - y_i \end{aligned} \quad (3.17)$$

Equation (2.35) is then applied with appropriate boundary conditions.

Planform symmetry is included by reflecting either the panel or control point about the x-axis and applying eq (2.35). Reflecting the control point is less complicated from a programming viewpoint.

The above process is repeated for each panel on the wing. After all the contributions to  $w_i$  have been calculated, it can be written as:

$$v_i = \sum_{j=1}^{2MN+M} A_{ij} \theta_j \quad (3.18)$$

where  $\theta_j$  is the column vector of unknown corner vorticities and the coefficients  $A_{ij}$  are functions of panel geometry. The  $\theta_j$  are numbered using the system given by eqs (3.9) through (3.16). One control point equation (3.18) is obtained for each panel on the wing and together they comprise  $MN$  conditions.

#### Edge Continuity Conditions

The  $\delta$  component of vorticity eq (2.7) is discontinuous across the panel diagonal (See discussion in Section II.). This can be partially remedied by specifying a point continuity condition at the panel lower right hand corner. This condition is:

$$\delta_L(x_4, y_2) = \delta_4 \quad (3.19)$$

which becomes

$$\begin{aligned} \delta_4 - \delta_3 + [(x_3 - x_4)/(y_2 - y_1)] \gamma_1 - \\ [(x_1 - x_4)/(y_2 - y_1)] \gamma_3 - [(x_3 - x_1)/ \\ (y_2 - y_1)] \gamma_4 = 0 \end{aligned} \quad (3.20)$$

after substituting of  $(x_4, y_2)$  and the expressions for  $C_L$  (2.13),  $E_L$  (2.16), and  $F_L$  (2.17) into eq (2.7). One condition eq (3.20) is formulated for each panel on the wing for a total of MN condition. Note that  $\delta$  is still not continuous across the panel diagonal due to the remaining discontinuity at the upper left hand corner. Also  $\delta$  is not continuous across panel side edges.

The edge continuity conditions and control point equations total 2MN conditions. M additional conditions can be obtained by specifying an edge continuity condition for  $\delta$  at the upper left hand corner of each panel along the centerline. This condition is

$$\delta_T(x_1, y_1) = \delta_1 \quad (3.21)$$

which becomes

$$\begin{aligned} \delta_2 - \delta_1 - [(x_2 - x_1)/(y_1 - y_2)] \gamma_4 + \\ [(x_4 - x_1)/(y_1 - y_2)] \gamma_2 + [(x_2 - x_4)/ \\ (y_1 - y_2)] \gamma_1 = 0 \end{aligned} \quad (3.22)$$

after substitution of  $(x_1, y_1)$  and the expressions for  $C_T$  (2.20),  $E_T$  (2.21), and  $F_T$  (2.22) into eq (2.7). This choice is based on trial and error, the additional  $\delta$  continuity on the centerline having the effect of minimizing vorticity oscillations.

#### Compressibility

Compressibility effects are accounted for by using the Prandtl-Glauert transformation (Ref 2:124-127):

$$\bar{x} = x / \sqrt{1 - M^2} \quad (3.23)$$

The transformation is applied to all  $x$  coordinates which are used in either the control point equations or edge continuity conditions.

#### Matrix Formulation

The control point equations and edge continuity conditions are  $2 MN + M$  equations in the unknowns,  $\theta_j$ . This system has the matrix formulation:

$$\begin{bmatrix} A_{ij} \end{bmatrix} \cdot \begin{bmatrix} \theta_1 \\ \theta_2 \\ \vdots \\ \theta_{2MN+M} \end{bmatrix} = \begin{bmatrix} v_1 \\ v_2 \\ \vdots \\ v_{MN} \\ 0 \end{bmatrix} \quad (3.24)$$

$(2MN + M) \times (2MN + M)$

The first  $MN$  rows of  $A_{ij}$  are the coefficients for the control point equations and are all nonzero. The last  $MN + M$  rows of  $A_{ij}$  correspond to the homogeneous edge continuity conditions and have no more than five nonzero entries per row.

#### Solution

The linearized form of the flow tangency boundary condition is (Ref 5:495):

$$v/v_\infty = dc/dx - \alpha \quad (3.25)$$

Where  $\alpha$  is the wing angle of attack,  $dc/dx$  is the local camber slope and  $v_\infty$  is the free stream velocity. This expression is substituted for each  $v_i$  in eq 3.24 where  $dc_i/dx$  is the panel slope at control point  $i$ . In matrix notation,

$$\begin{bmatrix} A_{ij} \end{bmatrix} \cdot \begin{bmatrix} \theta_j \end{bmatrix} = \begin{bmatrix} v_{\infty} (dc_1/dx - \alpha') \\ 0 \end{bmatrix} \quad (3.26)$$

or

$$\theta_j/v_{\infty} = \begin{bmatrix} A_{ij} \end{bmatrix}^{-1} \begin{bmatrix} dc_1/dx - \alpha' \\ 0 \end{bmatrix} \quad (3.27)$$

Forces and Moments

Once the  $\theta_j/v$  are obtained for a given  $\alpha'$  and camber slope distribution, eqs (2.3) and (2.7) can be used to calculate the vorticity strength at any point on the planform. The surface perturbation velocities in terms of local vorticity are (Ref 5:508):

$$u/v_{\infty} = \pm \gamma/2 \quad (3.28)$$

$$v/v_{\infty} = \mp \delta/2 \quad (3.29)$$

The upper sign corresponds to the upper wing surface and visa-versa.

Pressure coefficients are obtained from the perturbation velocities by either using the exact isentropic expression (Ref 3:167):

$$c_p = 2[(1 + (\gamma - 1)M_{\infty}^2)/2(1 - ((v_{\infty} + u)^2 + v^2 + w^2)/v_{\infty}^2) \gamma/(\gamma - 1) - 1]/(\gamma M_{\infty}^2) \quad (3.30)$$

or the second order approximation (Ref 3:167):

$$c_p = - [2u/v_{\infty} + (1 - M_{\infty}^2)u^2/v_{\infty}^2 + (v^2 + w^2)/v_{\infty}^2] \quad (3.31)$$

which is adequate for two-dimensional and planar flows. These coefficients are integrated along chord lines to obtain local lift and moment coefficients. The appropriate expressions are

$$c_L = (1/c) \int_{x_{LE}}^{x_{TE}} (c_{p_1} - c_{p_u}) dx \quad (3.32)$$

$$c_M = (1/c^2) \int_{x_{LE}}^{x_{TE}} (c_{p_1} - c_{p_u}) x dx \quad (3.33)$$

where the subscripts 1 and u refer to the lower and upper wing surfaces.

#### IV. Results

A FORTRAN Code "WING" was developed to analyze planform flow using the methodology discussed in Sections II and III. Most of the programming techniques used in WING were previously developed by the author and can be found in Reference 8.

Program WING was exercised for a variety of four point wings, taper ratios, and sweep angles. This section presents results for two of these wings.

Two general observations are made first. One, control point location is the major factor controlling bounded numerical oscillations of the vorticity vector as it is in many current paneling routines (ex. Refs 6 and 8). Oscillations are very common if the control point is located anywhere on the leading triangle. Fewer oscillations occur if the control point is located on the trailing triangle with  $.1 \leq CY \leq .5$  and  $.4 \leq CX \leq .9$ . Secondly, the program shows the best results when uniform spanwise paneling is used. Non-uniform spanwise paneling tends to cause oscillations in the vorticity vector. However, non-uniform chordwise paneling seems to have little effect on solution stability. The best total  $C_L$  match (with other known solutions) occurs at approximately  $CY = .15$  and  $CX = .75$ .

##### Rectangular Wing

The first case examined is a rectangular wing;  $AR = 8, \alpha = 5^\circ$  and  $M_\infty = .1$ . The wing is modeled using 11 uniformly spaced span stations and 6 non-uniformly spaced chord stations (0., .1, .3, .6,

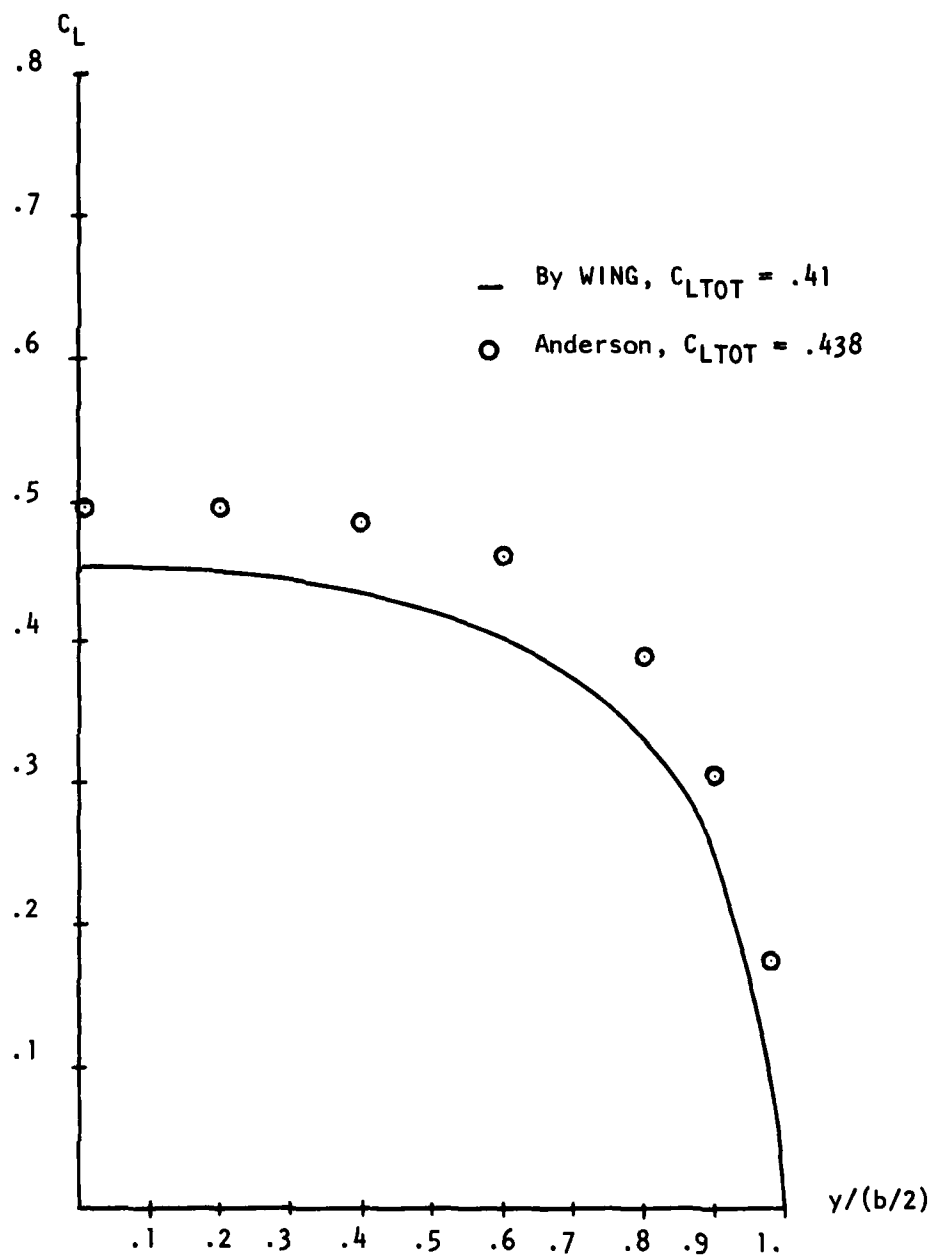


Figure 4.  $C_L$  Versus Span Station for a Rectangular Wing;  $AR = 8, \alpha = 5^\circ$

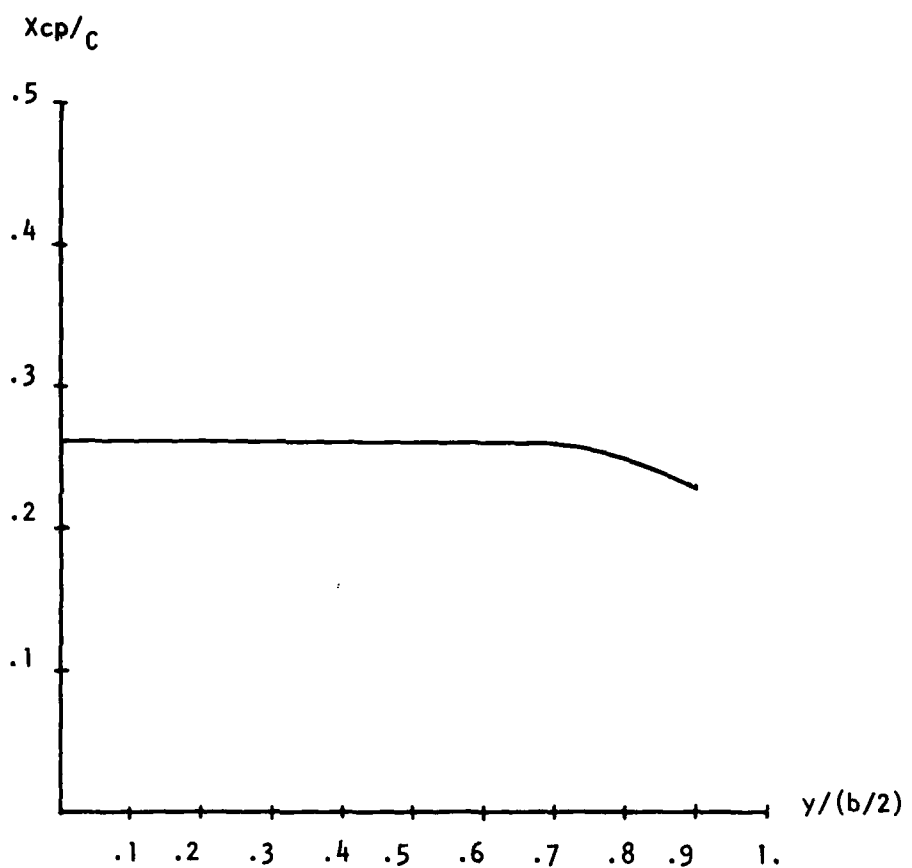


Figure 5.  $X_{CP}/C$  Versus Span Station for a  
Rectangular Wing;  $AR = 8, \alpha = 5^\circ$

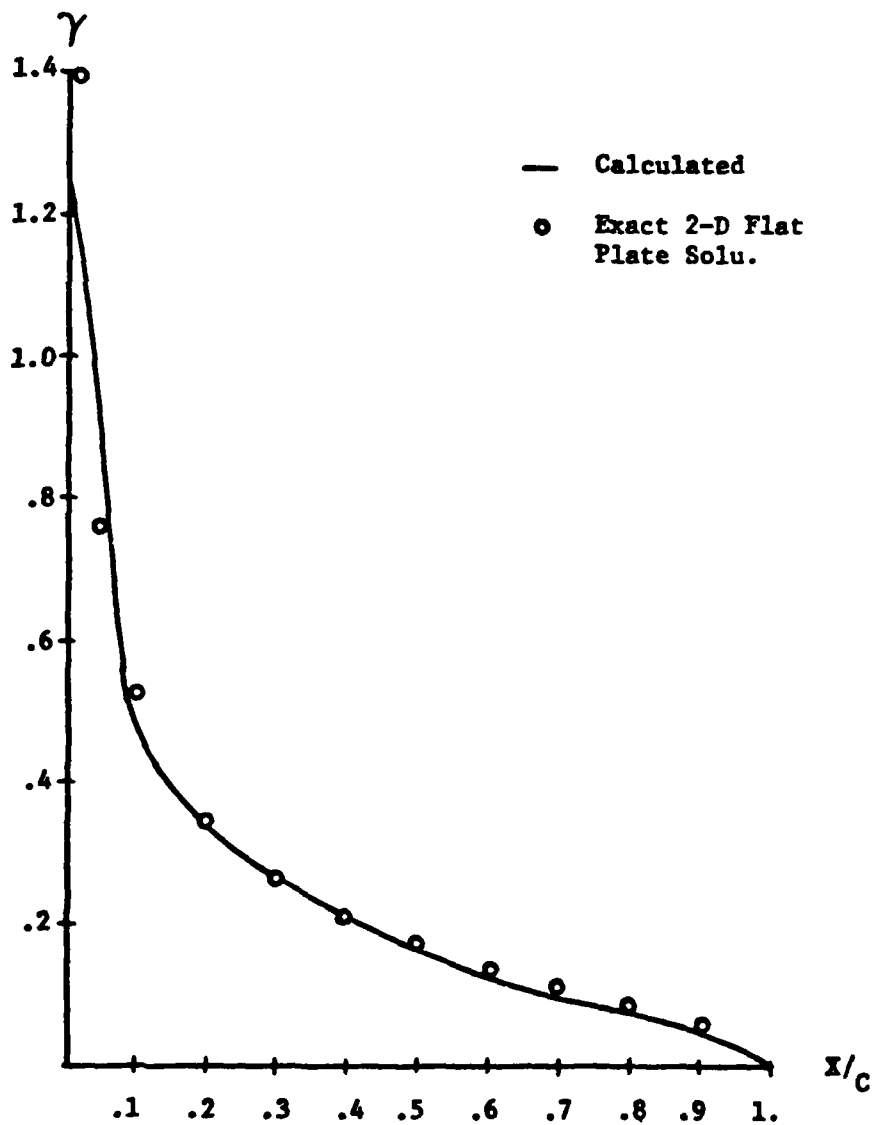


Figure 6.  $\gamma$  Strength Distribution at the Root Chord of a Rectangular Wing;  $AR = 8$ ,  $\alpha = 5^\circ$

.8, and 1.) which define 50 panels. Figure 4 shows the  $C_L$  distribution predicted by WING and Anderson (Ref 1:9-16). Figure 5 shows the spanwise distribution of center of pressure. The  $x_{cp}$  stays close to the classical 25% chord location except in the outboard region where it travels forward as expected.

Figure 6 is the  $\gamma$  strength at the root chord. The calculated solution compares favorably with the exact 2-D flat plate solution (Ref 5:515):

$$\gamma(x) = 2 \alpha (c - x)/(cx - x^2) \quad (5.1)$$

where  $c$  is the chord length and  $\alpha$  is measured in radians.

#### Swept Wing

The second case examined is a swept untapered wing;  $AR = 4.5$ ,  $\Lambda = 40^\circ$ ,  $\alpha = 5^\circ$ , and  $M_\infty = .1$ . The wing modeling is the same as the rectangular wing. Figure 7 shows the  $C_L$  distribution predicted by WING and by wind tunnel tests (Ref 4:92). Figure 8 shows the  $x$  center of pressure versus span station. Again, good agreement is obtained for both the  $C_L$  distribution and  $x_{cp}$  travel.

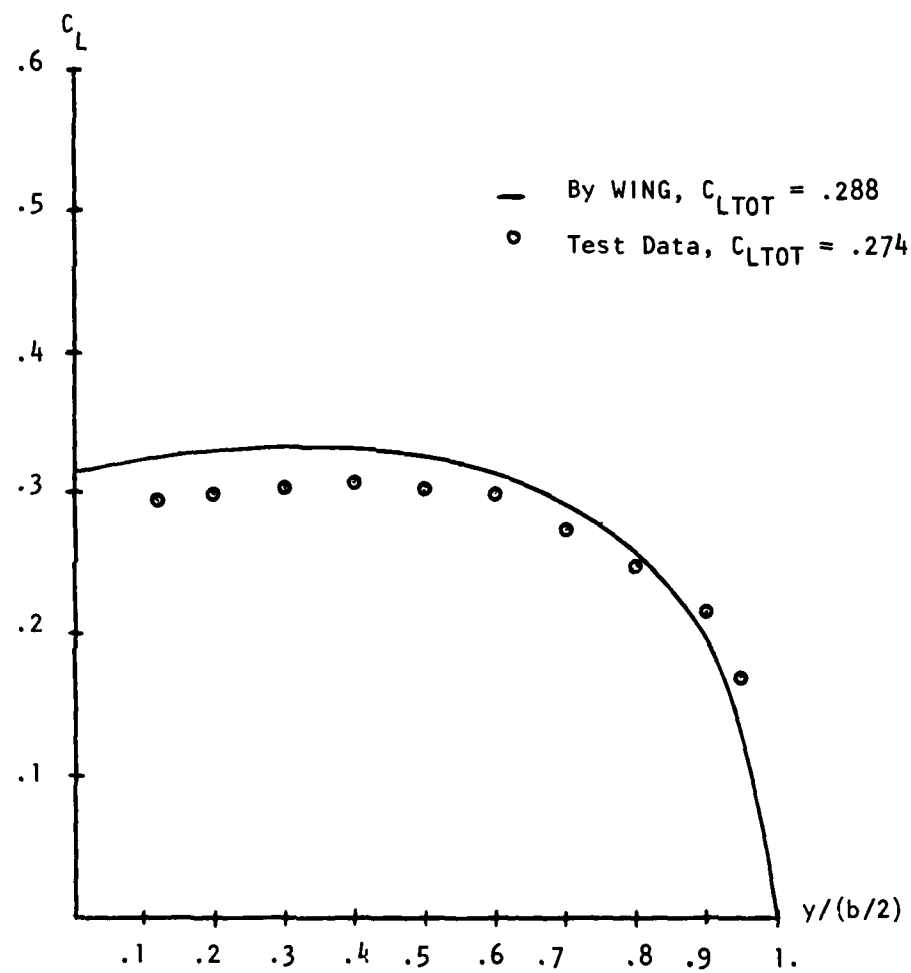


Figure 7.  $C_L$  Versus Span Station for a Sweptback Untapered Wing;  $AR = 4.5$ ,  $\Lambda = 40^\circ$ ,  $\alpha = 5^\circ$

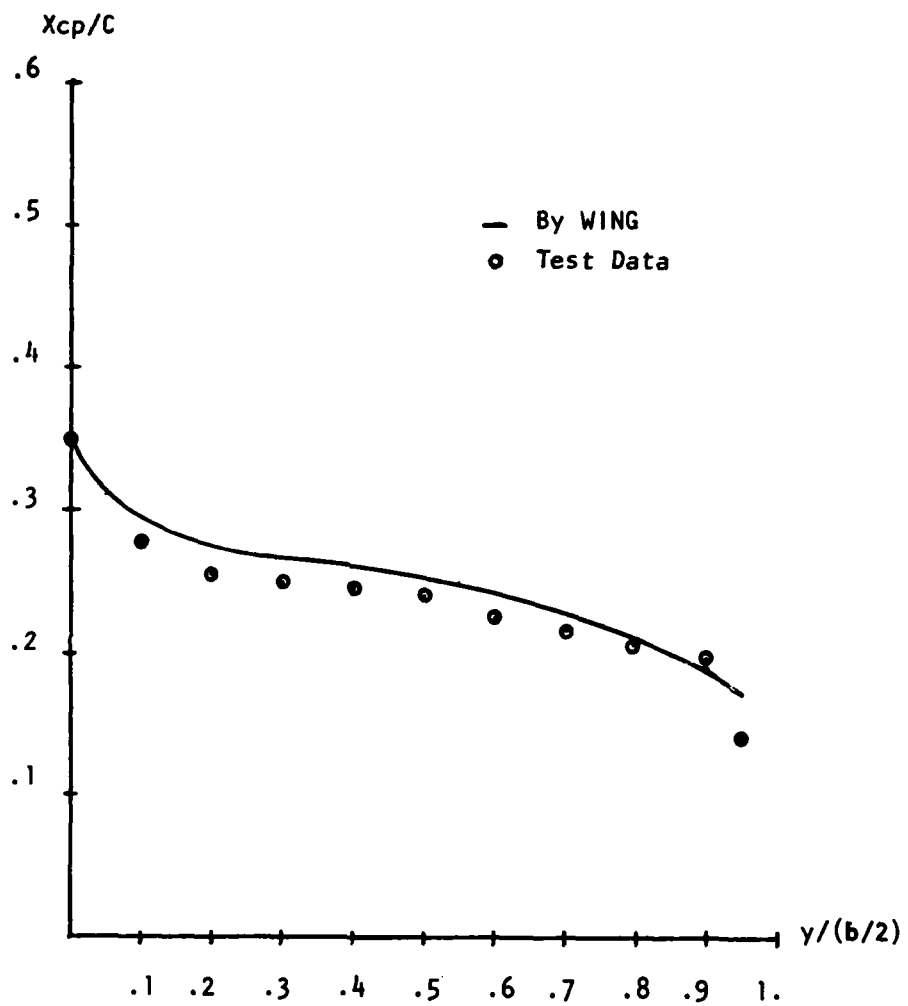


Figure 8.  $X_{cp}/C$  Versus Span Station for a Sweptback Untapered Wing;  $AR = 4.5$ ,  $\Lambda = 40^\circ$ ,  $\chi = 5^\circ$

V. Conclusions and Recommendations

Conclusions

A paneling technique which allows the vorticity vector to change direction has been demonstrated. The proper choice of control point (see section IV) will guarantee a solution free of numerical oscillations in the vorticity vector. This method has been implemented on a computer and introduces no new complexities to an experienced programmer. Existing mesh generators and other aerodynamic modules were incorporated into this technique (Ref 8). Computer run times are of the same order as programs incorporating "fixed direction" vorticity panels and no problems involving extensive "run times" were encountered.

The method gives satisfactory aerodynamic results for the cases examined. However, as in other paneling methods, the results are control point sensitive and some "curve fitting" is involved to find the control point location that best matches existing data or solutions. Also, the best "fits" don't show any appreciable improvement over existing paneling methods such as the constant strength vorticity panel program described in reference 8.

Recommendations

The following ideas are suggested for further study or improvement of the method:

- a. The method should be tested for cranked wings.
- b. The panel should be oriented in space to allow method assessment for three dimensional flow situations.

## APPENDIX A

Evaluation of the Panel Integrals

The methodology for evaluating the integrals  $I_i^{L,T}$  of section 2 is presented here.

Consider the semi-infinite region shown in Figure 9. This strip is bound by the lines  $y = y_0$ ,  $y = y_1$ , and the line segment connecting  $(x_0, y_0)$  to  $(x_1, y_1)$ . The equation for the line segment is:

$$y = Mx + b \quad (A.1)$$

where

$$M = (y_1 - y_0)/(x_1 - x_0) \quad (A.2)$$

and

$$b = y_0 - x_0 M \quad (A.3)$$

Define the following improper integrals on the semi-infinite strip

$$F_i = \lim_{L \rightarrow \infty} \int_{y_0}^{y_1} \int_{(y-b)/M}^L f_i(x, y) dx dy \quad (i = 1, \dots, 5) \quad (A.4)$$

where

$$f_1(x, y) = x/(x^2 + y^2)^{3/2} \quad (A.5)$$

$$f_2(x, y) = x^2/(x^2 + y^2)^{3/2} \quad (A.6)$$

ASD-TR-81-5005

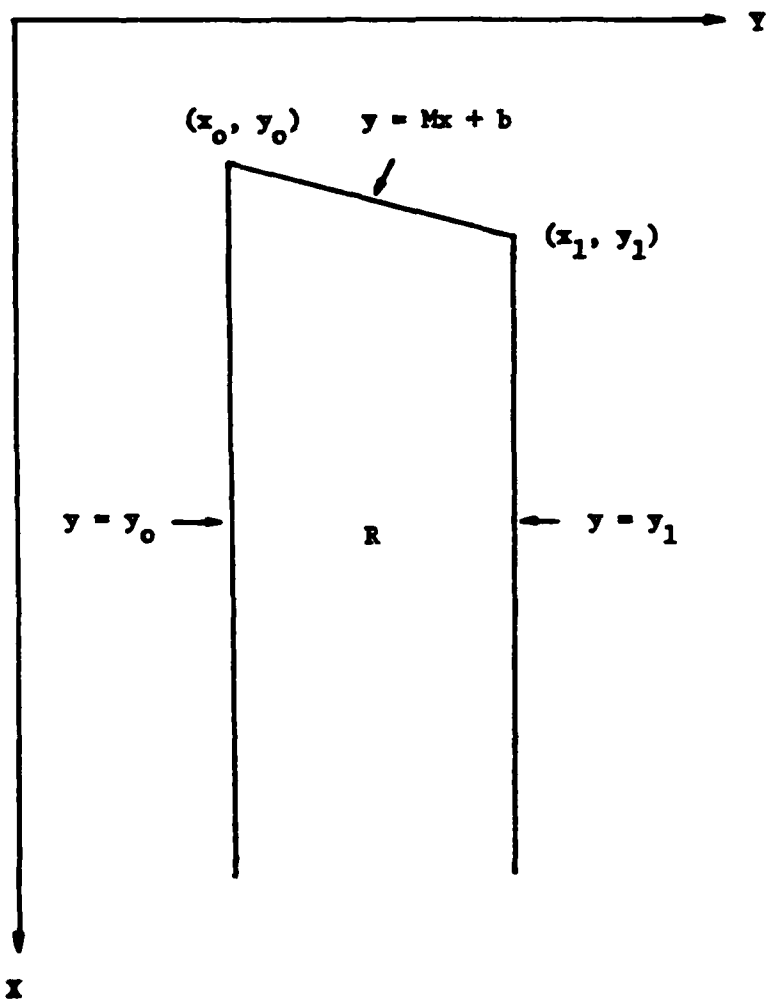


Figure 9. Semi-Infinite Strip  $R$  Used In Integral Evaluation

$$\xi_3(x, y) = xy/(x^2 + y^2)^{3/2} \quad (A.7)$$

$$\xi_4(x, y) = y/(x^2 + y^2)^{3/2} \quad (A.8)$$

and

$$\xi_5(x, y) = y^2/(x^2 + y^2)^{3/2} \quad (A.9)$$

To illustrate the methodology used in evaluating the integrals (A.4), consider

$$F_5 = \lim_{L \rightarrow \infty} \int_{y_0}^{y_1} \int_{(y-b)/M}^L [y^2/(x^2 + y^2)^{3/2}] dx dy \quad (A.10)$$

By Pierce's integral tables (Ref 7),

$$F_5 = \lim_{L \rightarrow \infty} \int_{y_0}^{y_1} [y^2 x / (y^2 \sqrt{x^2 + y^2})] \Big|_{(y-b)/M}^L dy = \quad (A.11)$$

$$\lim_{L \rightarrow \infty} \int_{y_0}^{y_1} L dy / \sqrt{L^2 + y^2} - \int_{y_0}^{y_1} ((y-b)/M) dy / \sqrt{((y-b)/M)^2 + y^2} \quad (A.12)$$

Substituting

$$z = (y-b)/M \quad (A.13)$$

and

$$dy = M dz \quad (A.14)$$

ASD-TR-81-5005

into the rightmost integral of (A.12) yields:

$$F_5 = \lim_{L \rightarrow \infty} \int_{y_0}^{y_1} \left( L dy / \sqrt{L^2 + y^2} \right) - M \int_{x_0}^{x_1} zdz / \sqrt{z^2 + (Mz + b)^2} \quad (A.15)$$

The integrals (A.15) can be evaluated using Ref. 7. One obtains, after some algebraic manipulation,

$$\begin{aligned} F_5 = & \lim_{L \rightarrow \infty} L \ln[(y_1 + \sqrt{y_1^2 + L^2}) / (y_0 + \sqrt{y_0^2 + L^2})] + \\ & [bM^2 / (1 + M^2)^{3/2}] \ln[(\sqrt{x_1^2 + y_1^2} + ((x_1 + My_1) / \sqrt{1 + M^2})) / \\ & (\sqrt{x_0^2 + y_0^2} + ((x_0 + My_0) / \sqrt{1 + M^2}))] + \\ & [M / (1 + M^2)] (\sqrt{x_0^2 + y_0^2} - \sqrt{x_1^2 + y_1^2}) \end{aligned} \quad (A.16)$$

recalling

$$y_0 = Mx_0 + b \quad (A.17)$$

and

$$y_1 = Mx_1 + b \quad (A.18)$$

Notice the limit

$$\lim_{L \rightarrow \infty} L \ln[(y_1 + \sqrt{y_1^2 + L^2}) / (y_0 + \sqrt{y_0^2 + L^2})] \quad (A.19)$$

is not a function of  $x_0$  or  $x_1$  which leads to the following observation. If the integral  $F_5$  is evaluated on any other semi-infinite strip bounded by the lines  $y = y_0$  and  $y = y_1$ , the limit (A.19) is invariant. Evaluating the integral  $F_5$  using any other line segment connecting  $y = y_0$  to  $y = y_1$  and formulating the difference between this result and (A.16) leads to cancellation of the limit (A.19).

The other four integrals,  $F_1$  through  $F_4$ , can be evaluated by a similiar procedure using Ref 7. Each integral has a limit term given by:

$$(F_1) \lim_{L \rightarrow \infty} \ln[(y_0 + \sqrt{y_0^2 + L^2})/(y_1 + \sqrt{y_1^2 + L^2})] \quad (A.20)$$

$$(F_2) \lim_{L \rightarrow \infty} [y_1 \ln(\sqrt{L^2 + y_1^2} + L) - y_0 \ln(\sqrt{L^2 + y_0^2} + L)] \quad (A.21)$$

$$(F_3) \lim_{L \rightarrow \infty} [\sqrt{L^2 + y_0^2} - \sqrt{L^2 + y_1^2}] \quad (A.22)$$

$$(F_4) \lim_{L \rightarrow \infty} \ln[(L + \sqrt{L^2 + y_0^2})/(L + \sqrt{L^2 + y_1^2})] \quad (A.23)$$

These terms cancel upon the formulation of integral differences.

Retaining the finite terms from each of the integral evaluations, we can define "Strip Functions"  $S_i$  for the functions  $f_i$  and the points  $(x_0, y_0)$  and  $(x_1, y_1)$  by

$$S_i[(x_0, y_0), (x_1, y_1)] = (M/\sqrt{1 + M^2})c \quad (A.24)$$

$$s_2[(x_0, y_0), (x_1, y_1)] = y_0 \ln[\sqrt{x_0^2 + y_0^2} + x_0] - \\ y_1 \ln[\sqrt{x_1^2 + y_1^2} + x_1] + (M/(1 + M^2))H + \\ [b/(1 + M^2)^{3/2}]G \quad (A.25)$$

$$s_3[(x_0, y_0), (x_1, y_1)] = (M^2/(1 + M^2))H + \\ [bM/(1 + M^2)^{3/2}]G \quad (A.26)$$

$$s_4[(x_0, y_0), (x_1, y_1)] = \ln[(x_1 + \sqrt{x_1^2 + y_1^2})/ \\ (x_0 + \sqrt{x_0^2 + y_0^2})] - G/\sqrt{1 + M^2} \quad (A.27)$$

$$s_5[(x_0, y_0), (x_1, y_1)] = [bM^2/(1 + M^2)^{3/2}]G - \\ (M/(1 + M^2))H \quad (A.28)$$

where

$$G = \ln[(\sqrt{x_1^2 + y_1^2} + ((x_1 + My_1)/\sqrt{1 + M^2}))/ \\ (\sqrt{x_0^2 + y_0^2} + ((x_0 + My_0)/\sqrt{1 + M^2}))] \quad (A.29)$$

and

$$H = \sqrt{x_1^2 + y_1^2} - \sqrt{x_0^2 + y_0^2} \quad (A.30)$$

Examining Figure 1, it is obvious that each of the panel integrals (2.30) through (2.34) can be obtained by formulating the difference of

two corresponding strip functions. This leads to the following fundamental results:

$$I_1^L = S_1[(x_1, y_1), (x_3, y_2)] - S_1[(x_1, y_1), (x_4, y_2)] \quad (A.31)$$

$$I_1^T = S_1[(x_1, y_1), (x_4, y_2)] - S_1[(x_2, y_1), (x_4, y_2)] \quad (A.32)$$

where  $i$  ranges from 1 to 5.

## APPENDIX B

Simple Wake Model

The Kutta condition (Ref 5:390-399) implies

$$\vec{\omega}(x, y) = \delta(x, y) \hat{i} \quad (B.1)$$

for all points on the wing trailing edge. Let vortex filaments emanate from corners 2 and 4 of a trailing edge panel and extend to infinity (see Figure 10). By Helmholtz's theorems, these filaments will retain the strengths  $\delta_2$  and  $\delta_4$  indefinitely. Now assume that the strength of the wake region between the two filaments is given by:

$$\delta(x, y) = (My + b) \hat{i} \quad (B.2)$$

where

$$M = (\delta_4 - \delta_2)/(y_2 - y_1) \quad (B.3)$$

$$b = \delta_2 - y_1[(\delta_4 - \delta_2)/(y_2 - y_1)] \quad (B.4)$$

Applying the Biot-Savart Law (Section 11), the effect of the wake region upon the induced velocity at a control point located at the origin of the coordinate system is

$$4\pi T_w = -M S_5[(x_2, y_1), (x_4, y_2)] - b S_4[(x_2, y_1), (x_4, y_2)] \quad (B.5)$$

The limit terms (A.23) and (A.19) for the "Strip Functions"  $S_4$  and  $S_5$  must now be evaluated and

$$(S_4) \lim_{L \rightarrow \infty} L \ln \left[ (L + \sqrt{L^2 + y_1^2}) / (L + \sqrt{L^2 + y_2^2}) \right] = 0 \quad (B.6)$$

$$(S_5) \lim_{L \rightarrow \infty} L \ln \left[ (y_2 + \sqrt{y_2^2 + L}) / (y_1 + \sqrt{y_1^2 + L}) \right] = y_2 - y_1 \quad (B.7)$$

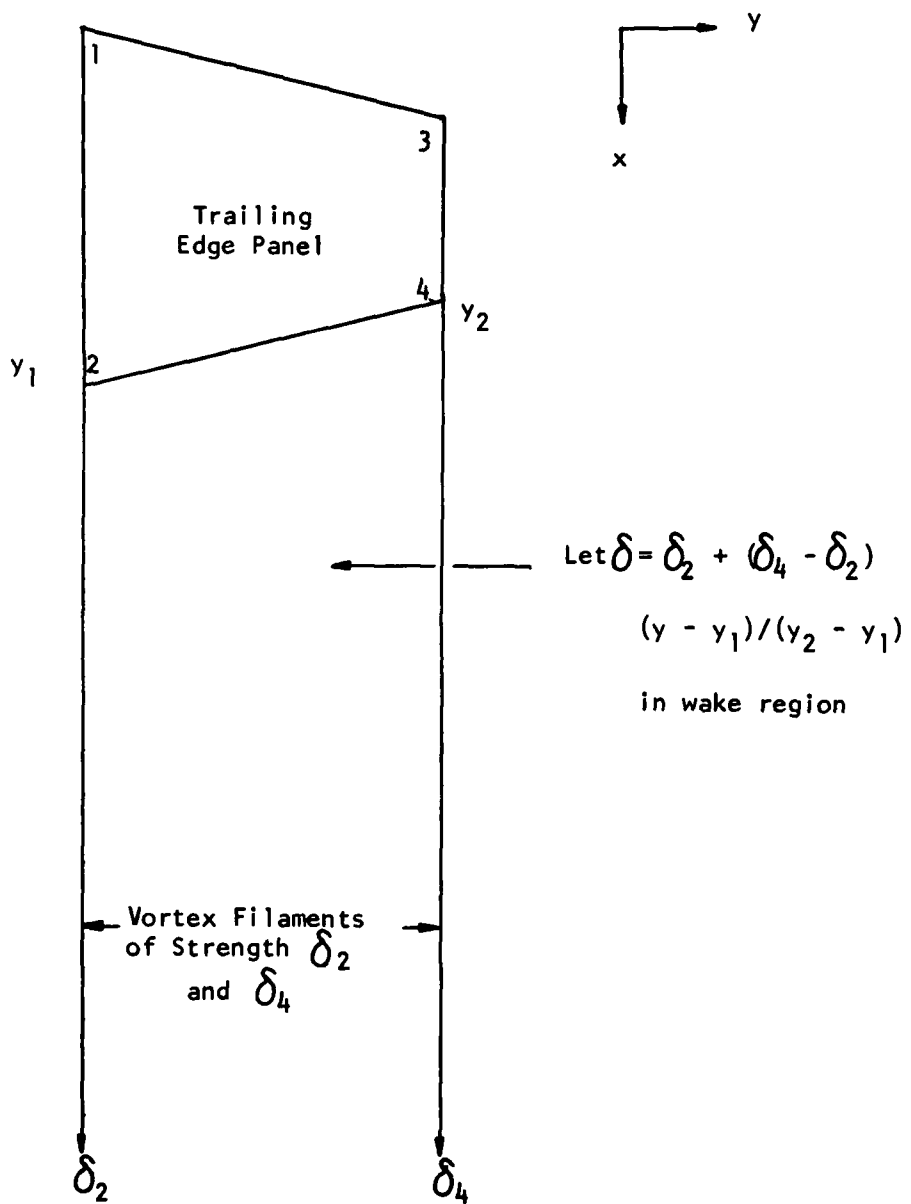


Figure 10. Wake Model

Collecting coefficients of  $\delta_2$  and  $\delta_4$ , we obtain

$$4\pi T W = [(s_5 - y_2 s_4)/(y_2 - y_1)] \delta_2 + [(y_1 s_4 - s_5)/(y_2 - y_1)] \delta_4 \quad (B.8)$$

which is the induced velocity at a point due to a wake region emanating behind an arbitrary trailing edge panel.

Bibliography

1. Abbot, Ira H. and von Doenhoff, Albert E. Theory of Wing Sections. New York: Dover Publications Inc., 1959.
2. Ashley, Holt and Landahl, Marten. Aerodynamics of Wings and Bodies. Reading, Massachusetts: Addison-Wesley Publishing Company, Inc., 1965.
3. Hughes, William F. and Brighton, John A. Schaum's Outline Series: Fluid Dynamics. New York: McGraw-Hill Book Company, 1967.
4. Jones, Robert T. and Cohen, Doris. High Speed Wing Theory. Princeton: Princeton University Press, 1960.
5. Karamcheti, Krishnamurty. Principles of Ideal-Fluid Aerodynamics. New York: John Wiley and Sons, Inc., 1966.
6. Minter, E. A. and Rudnicki, A. R. Preliminary Structural Design Load Prediction Techniques for Military Aircraft, Volume II. AFFDL-TR-76-23. Wright-Patterson Air Force Base, Ohio: Air Force Flight Dynamics Laboratory, February 1976.
7. Pierce, B. O. A Short Table of Integrals. New York: Ginn and Company, 1929.
8. Sparks, John C. A Calculator Program for Analyzing Airloads on a Wing of Arbitrary Planform and Camber in Subsonic Flow. AFFDL-TR-77-136. Wright-Patterson Air Force Base, Ohio: Air Force Flight Dynamics Laboratory, January 1978.
9. Yen, A.; Mook, D. T.; and Nayfeh, A. H. "Nonlinear Continuous - Vorticity Aerodynamics Model." AIAA 18th Aerospace Sciences Meeting. Pasadena, California: American Institute of Aeronautics and Astronautics, January 1980.